

Supplemental Information

Formation of ssDNA nanotubes from spherical micelles and their use as a delivery vehicle for chemotherapeutics and senolytics to triple negative breast cancer cells

Lucy Lin,^{a,b} Zachary Schneiderman,^{a,b} Aditya Venkatraman,^{a,b} and Efrosini Kokkoli*^{a,b}

^aDepartment of Chemical and Biomolecular Engineering, Johns Hopkins University, Baltimore, MD 21218, USA. E-mail: kokkoli@jhu.edu

^bInstitute for NanoBioTechnology, Johns Hopkins University, Baltimore, MD 21218, U.S.A.

*E-mail: kokkoli@jhu.edu

Table S1 Masses of ssDNA-amphiphiles as determined by MALDI-TOF

ssDNA-amphiphiles	Expected mass (Da)	Measured mass (Da)
ssDNA-amphiphile	4161.6	4166.4
HEX-labeled ssDNA-amphiphile	4905.7	4912.1

Table S2 Endocytic inhibitors with their targets and concentrations

Target	Inhibitor	Concentration (µg/mL)
Scavenger receptors	Fucoidan	500
Macropinocytosis	Dimethyl amiloride (DMA)	30, 60 ^a
Cytoskeleton	Latrunculin B (LatB)	1.6, 4 ^a
	Nocodazole	15
Caveolae/lipid rafts	Filipin	5
	MBCD	1320
	Nystatin	2.5
Clathrin	Chlorpromazine	2.5
	Dynasore	12.5
G-protein-coupled receptors (GPCRs)	Cholera toxin (CTX)	2
	Pertussis toxin (PTX)	0.2

^aSum159 required higher concentrations of inhibitors DMA and LatB to achieve inhibition.

Table S3 Statistical analysis comparing viability of cells after treatment with different groups^a

Group 1	Group 2	p-value
Cell Control	DOX-NT, 3d	0.0018
Cell Control	ABT-NT, 3d	0.0806
Cell Control	ABT-NT, ABT-NT, 3d	9.24E-06
Cell Control	ABT-NT, DOX-NT, 3d	2.02E-06
Cell Control	ABT-NT, ABT-NT+DOX-NT, 3d	3.16E-08
Cell Control	DOX-NT, 7d	8.20E-05
Cell Control	ABT-NT, 7d	0.00012
Cell Control	ABT-NT, ABT-NT, 7d	7.77E-07
Cell Control	ABT-NT, DOX-NT, 7d	2.23E-08
Cell Control	ABT-NT, ABT-NT+DOX-NT, 7d	8.50E-10
DOX-NT, 3d	ABT-NT, 3d	0.8163
DOX-NT, 3d	ABT-NT, ABT-NT, 3d	0.4282
DOX-NT, 3d	ABT-NT, DOX-NT, 3d	0.1297
DOX-NT, 3d	ABT-NT, ABT-NT+DOX-NT, 3d	0.0011
DOX-NT, 3d	DOX-NT, 7d	0.9451
DOX-NT, 3d	ABT-NT, 7d	0.9770
DOX-NT, 3d	ABT-NT, ABT-NT, 7d	0.0499
DOX-NT, 3d	ABT-NT, DOX-NT, 7d	0.0007
DOX-NT, 3d	ABT-NT, ABT-NT+DOX-NT, 7d	8.13E-06
ABT-NT, 3d	ABT-NT, ABT-NT, 3d	0.0170
ABT-NT, 3d	ABT-NT, DOX-NT, 3d	0.0032
ABT-NT, 3d	ABT-NT, ABT-NT+DOX-NT, 3d	2.27E-05
ABT-NT, 3d	DOX-NT, 7d	0.1360
ABT-NT, 3d	ABT-NT, 7d	0.1861
ABT-NT, 3d	ABT-NT, ABT-NT, 7d	0.0011
ABT-NT, 3d	ABT-NT, DOX-NT, 7d	1.48E-05
ABT-NT, 3d	ABT-NT, ABT-NT+DOX-NT, 7d	2.63E-07
ABT-NT, ABT-NT, 3d	ABT-NT, DOX-NT, 3d	0.9995
ABT-NT, ABT-NT, 3d	ABT-NT, ABT-NT+DOX-NT, 3d	0.1785
ABT-NT, ABT-NT, 3d	DOX-NT, 7d	0.9934
ABT-NT, ABT-NT, 3d	ABT-NT, 7d	0.9791
ABT-NT, ABT-NT, 3d	ABT-NT, ABT-NT, 7d	0.9745
ABT-NT, ABT-NT, 3d	ABT-NT, DOX-NT, 7d	0.1243
ABT-NT, ABT-NT, 3d	ABT-NT, ABT-NT+DOX-NT, 7d	0.0016
ABT-NT, DOX-NT, 3d	ABT-NT, ABT-NT+DOX-NT, 3d	0.5320
ABT-NT, DOX-NT, 3d	DOX-NT, 7d	0.8035
ABT-NT, DOX-NT, 3d	ABT-NT, 7d	0.7077
ABT-NT, DOX-NT, 3d	ABT-NT, ABT-NT, 7d	1.0000
ABT-NT, DOX-NT, 3d	ABT-NT, DOX-NT, 7d	0.4155
ABT-NT, DOX-NT, 3d	ABT-NT, ABT-NT+DOX-NT, 7d	0.0085
ABT-NT, ABT-NT+DOX-NT, 3d	DOX-NT, 7d	0.0236
ABT-NT, ABT-NT+DOX-NT, 3d	ABT-NT, 7d	0.0161
ABT-NT, ABT-NT+DOX-NT, 3d	ABT-NT, ABT-NT, 7d	0.8137
ABT-NT, ABT-NT+DOX-NT, 3d	ABT-NT, DOX-NT, 7d	1.0000
ABT-NT, ABT-NT+DOX-NT, 3d	ABT-NT, ABT-NT+DOX-NT, 7d	0.5348
DOX-NT, 7d	ABT-NT, 7d	1.0000
DOX-NT, 7d	ABT-NT, ABT-NT, 7d	0.5197
DOX-NT, 7d	ABT-NT, DOX-NT, 7d	0.0152
DOX-NT, 7d	ABT-NT, ABT-NT+DOX-NT, 7d	0.0002
ABT-NT, 7d	ABT-NT, ABT-NT, 7d	0.4179
ABT-NT, 7d	ABT-NT, DOX-NT, 7d	0.0103
ABT-NT, 7d	ABT-NT, ABT-NT+DOX-NT, 7d	0.0001
ABT-NT, ABT-NT, 7d	ABT-NT, DOX-NT, 7d	0.7051
ABT-NT, ABT-NT, 7d	ABT-NT, ABT-NT+DOX-NT, 7d	0.0249
ABT-NT, DOX-NT, 7d	ABT-NT, ABT-NT+DOX-NT, 7d	0.6567

^ap-values from one-way ANOVA with post-hoc Tukey's HSD test analysis of data shown in Fig. 4F.

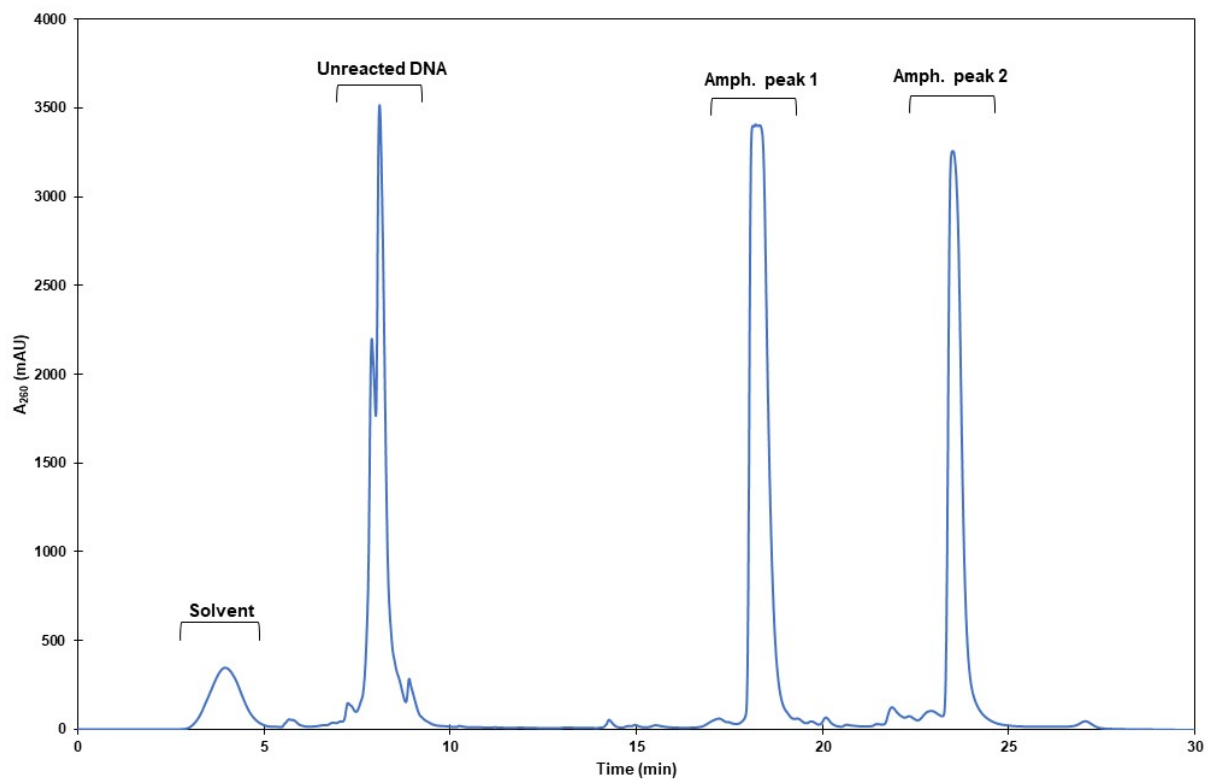


Fig. S1 Representative HPLC chromatogram from purification of ssDNA-amphiphiles.

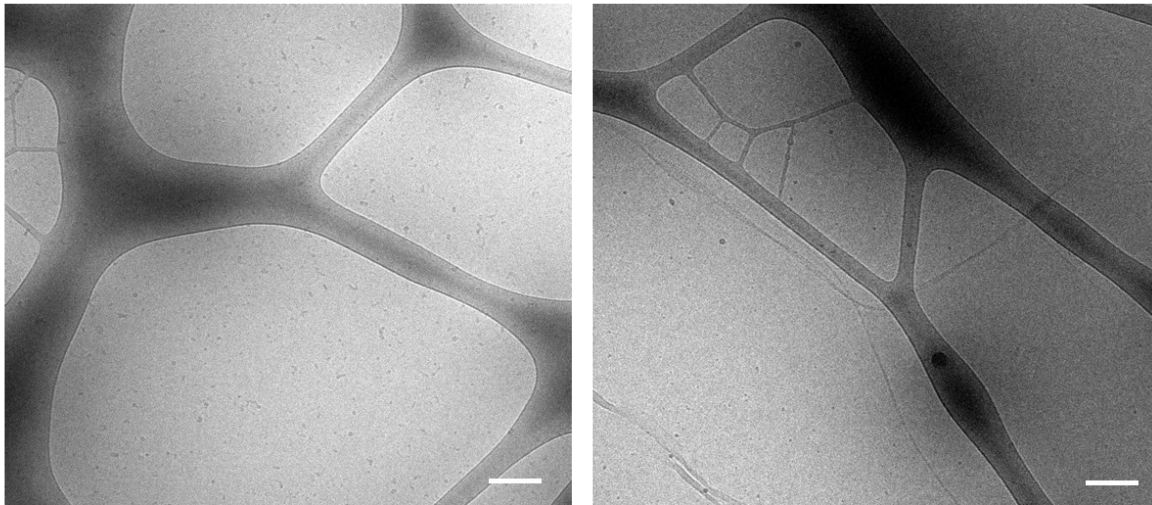
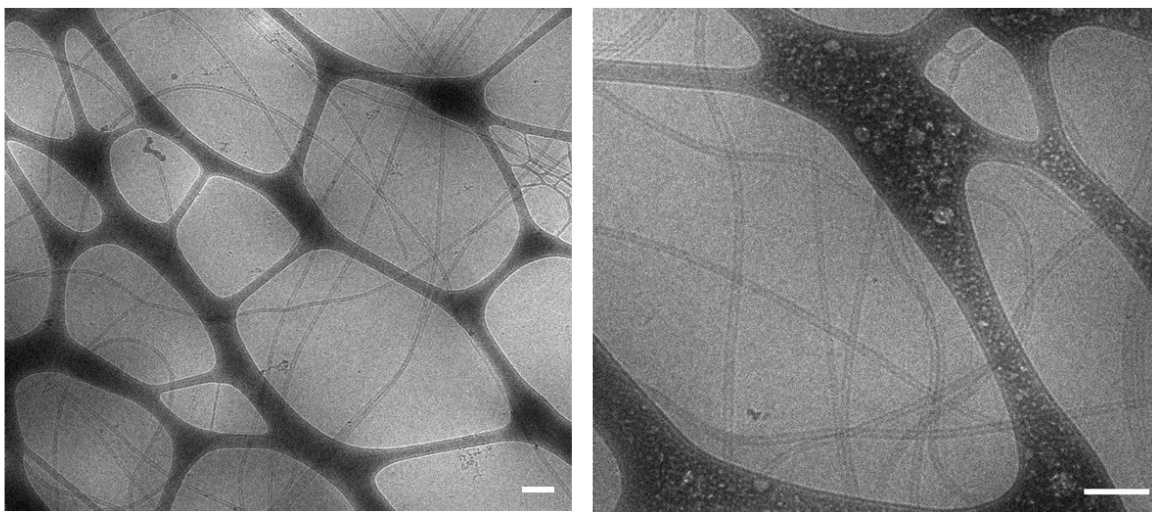
A**B**

Fig. S2 Peaks 1 and 2 from HPLC purification of ssDNA-amphiphiles were combined and purified via TFF. The permeate (A) and retentate (B) were imaged via cryo-TEM and representative images of each are shown. The permeate contained many micelles and a few twisted nanotapes, while the retentate contained nanotubes. Scale bars are 200 nm.

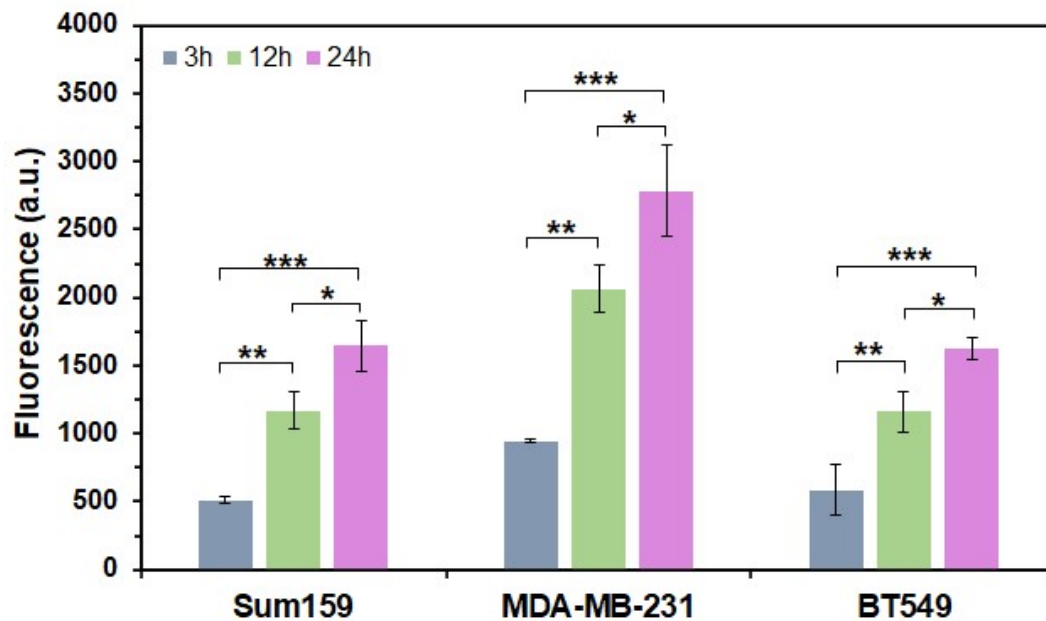


Fig. S3 Flow cytometry shows time dependent increase in cell association between the ssDNA nanotubes (5 nmol of 20% HEX-labeled nanotubes, 10 μ M total ssDNA-amphiphiles) and TNBC cells. Cell autofluorescence was subtracted from all data. Data are shown as mean \pm SD (n = 3). Statistical significance was assessed via one-way ANOVA with Tukey's HSD post-hoc analysis; * p < 0.05, ** p < 0.01, *** p < 0.001.

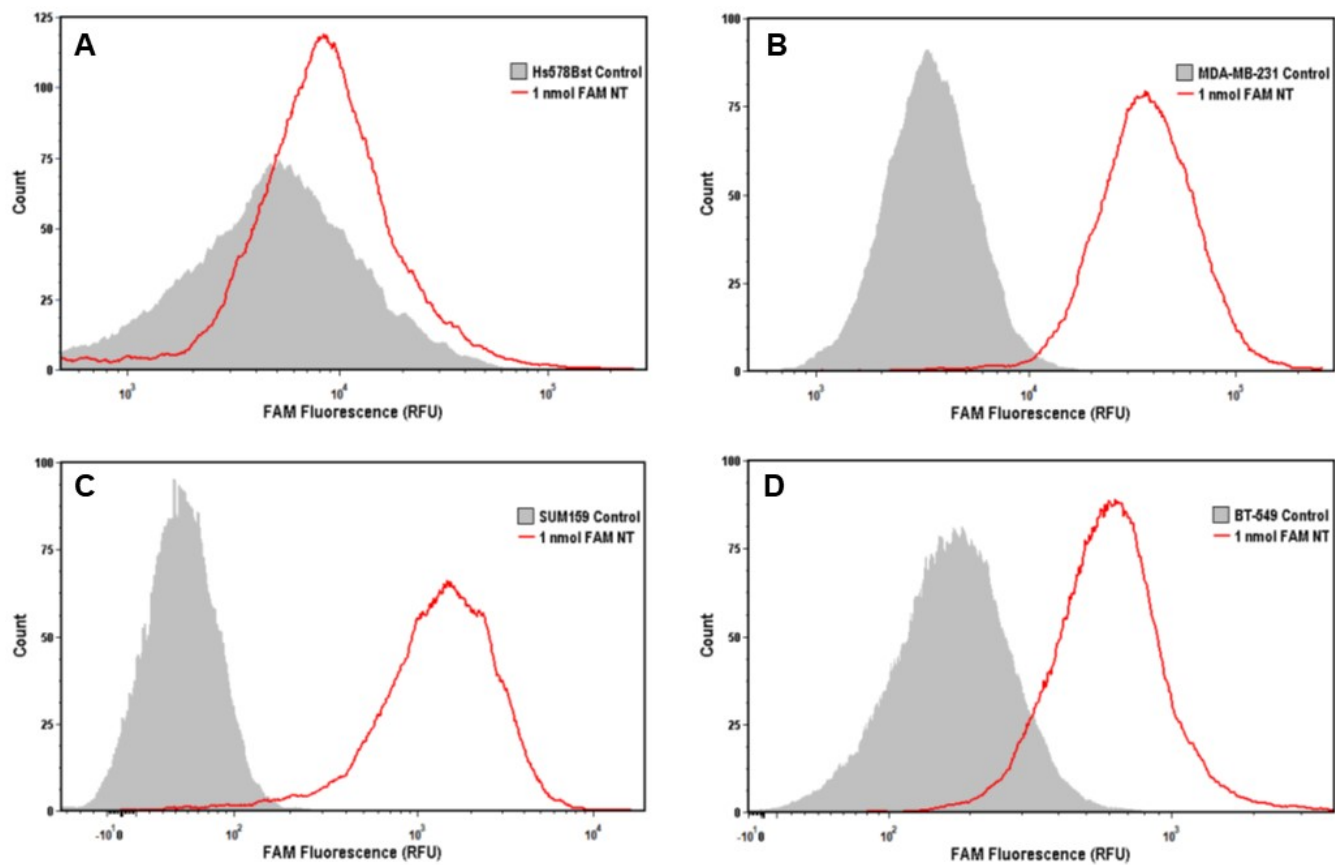


Fig. S4 Flow cytometry graphs showing association of ssDNA nanotubes (1 nmol of 100% FAM-labeled nanotubes) with (A) healthy Hs578Bst breast cells, and TNBC cells (B) MDA-MB-231, (C) Sum159 and (D) BT549, after 3 h incubation at 37 °C.

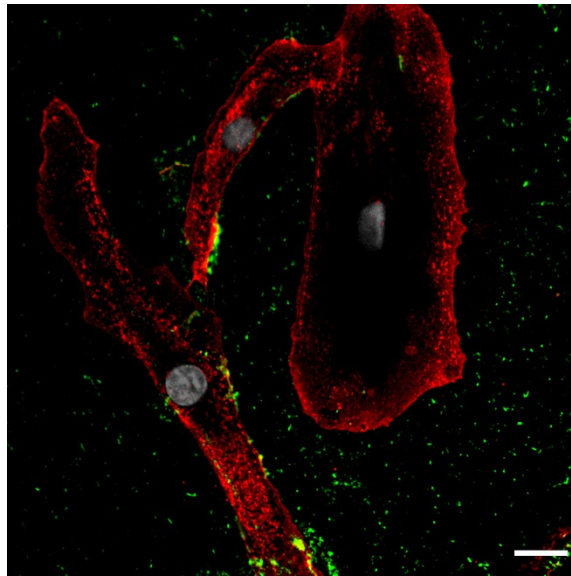


Fig. S5 Representative confocal image showing minimal internalization of 20% HEX-labeled nanotubes (green) in healthy Hs578Bst cells after 24 h at 37 °C. Cell membranes are labeled red and nuclei gray. Scale bar is 20 μm .

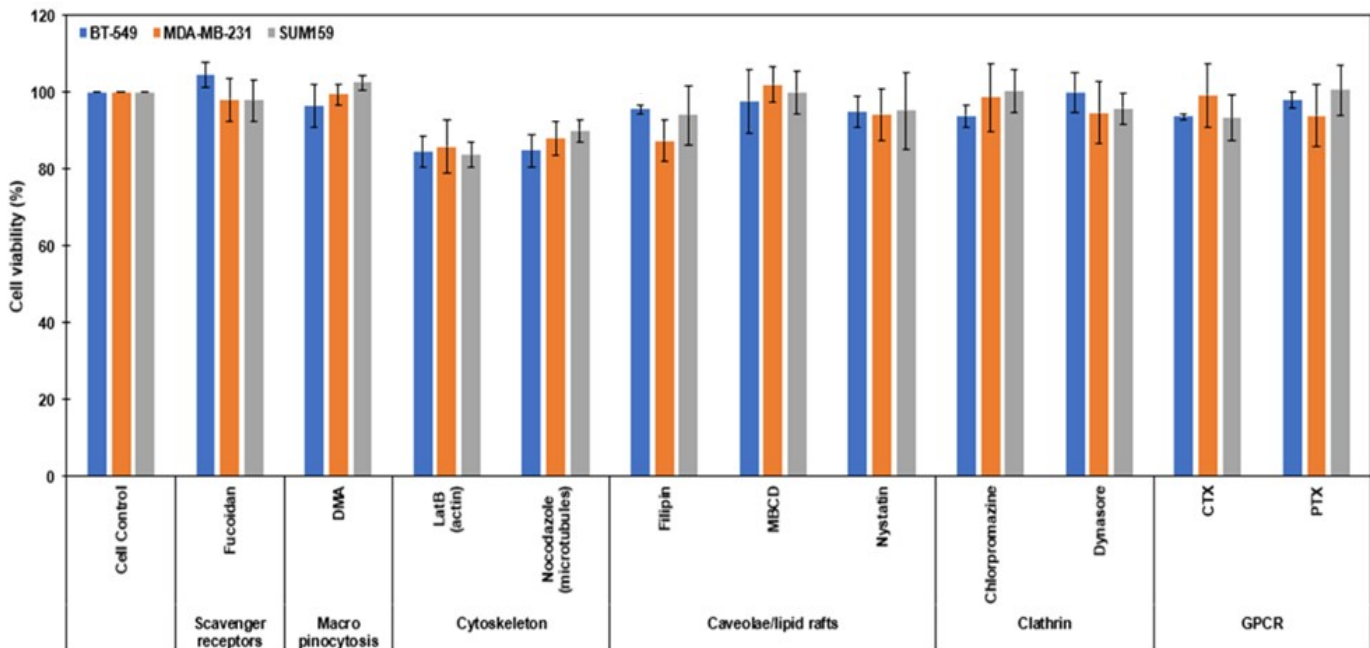


Fig. S6 Cytotoxicity of inhibitors after 3 h for the three TNBC cell lines. Data are shown as mean \pm SD ($n = 3$).

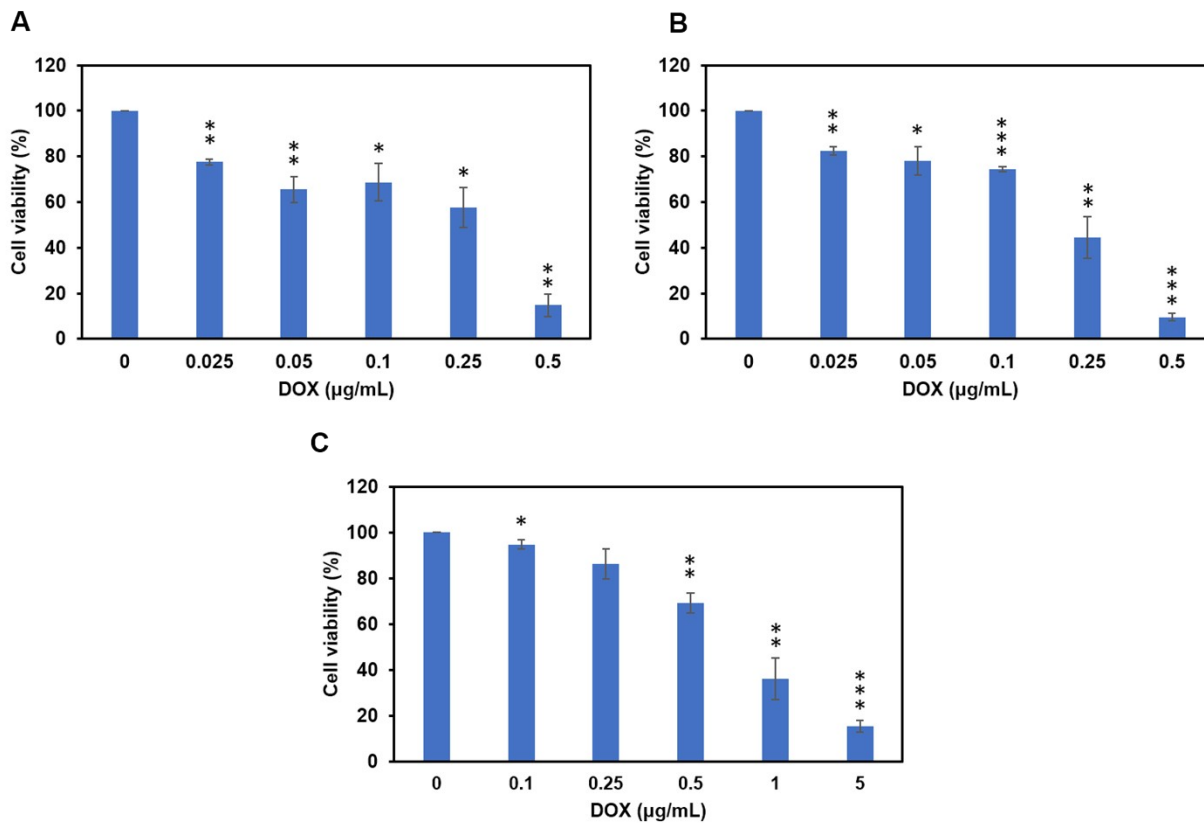


Fig. S7 Cytotoxicity of free DOX delivered to three TNBC cell lines: (A) Sum159, (B) BT549, and (C) MDA-MB-231. Note that MDA-MB-231 cells showed slight resistance to DOX so higher concentrations were used. Cells were treated with DOX for 12 h, washed, and let grow in fresh media for another 36 h at 37 °C. Data are shown as mean \pm SD ($n = 3$). Statistical significance was assessed between the DOX treatments and the control (0 μ M DOX) using a two-tailed unpaired t -test; * $p < 0.05$ ** $p < 0.01$ *** $p < 0.001$. All other results were not statistically significant, $p > 0.05$.

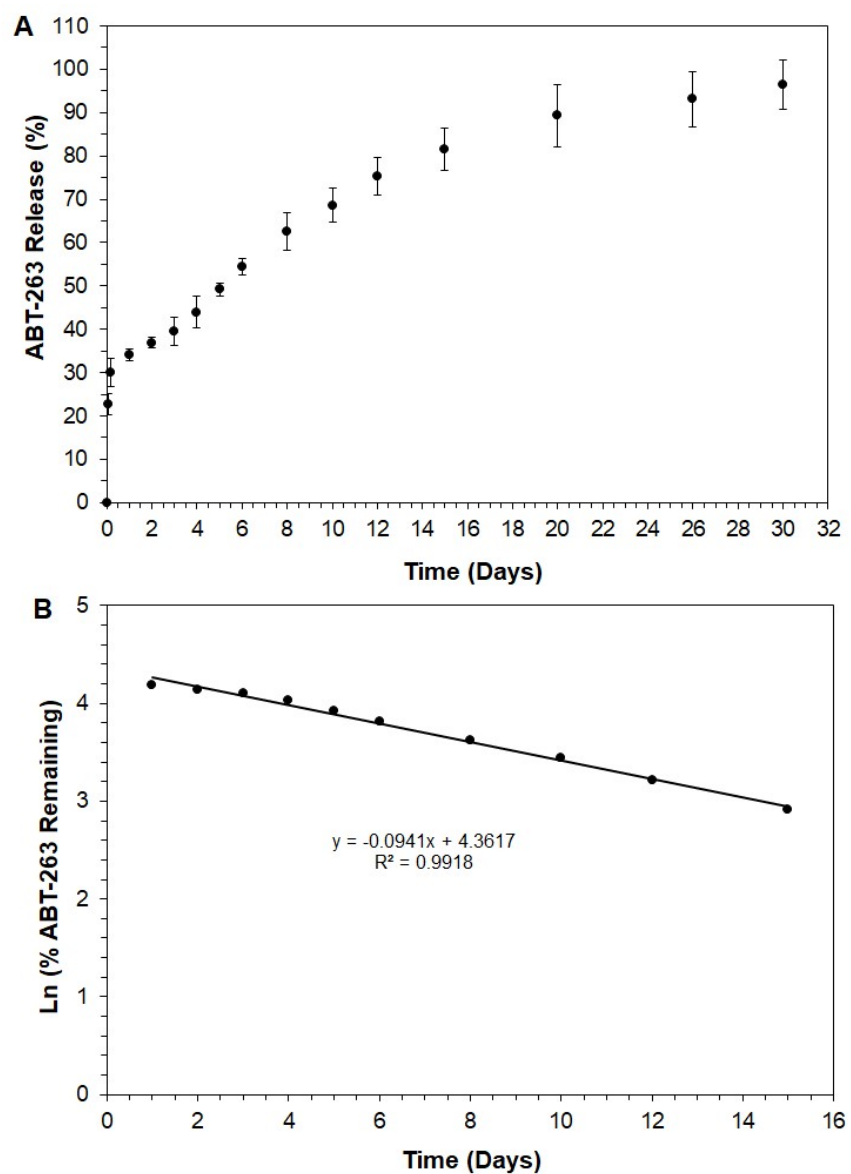


Fig. S8 (A) Cumulative release profile of ABT-263 from ssDNA nanotubes in PBS at 37 °C. Results are reported as mean \pm SD (n = 3 - 4). (B) Data from (A) plotted as Ln cumulative percentage of ABT-263 remaining in the nanotubes vs. time, demonstrating first-order release kinetics on day 1-15.

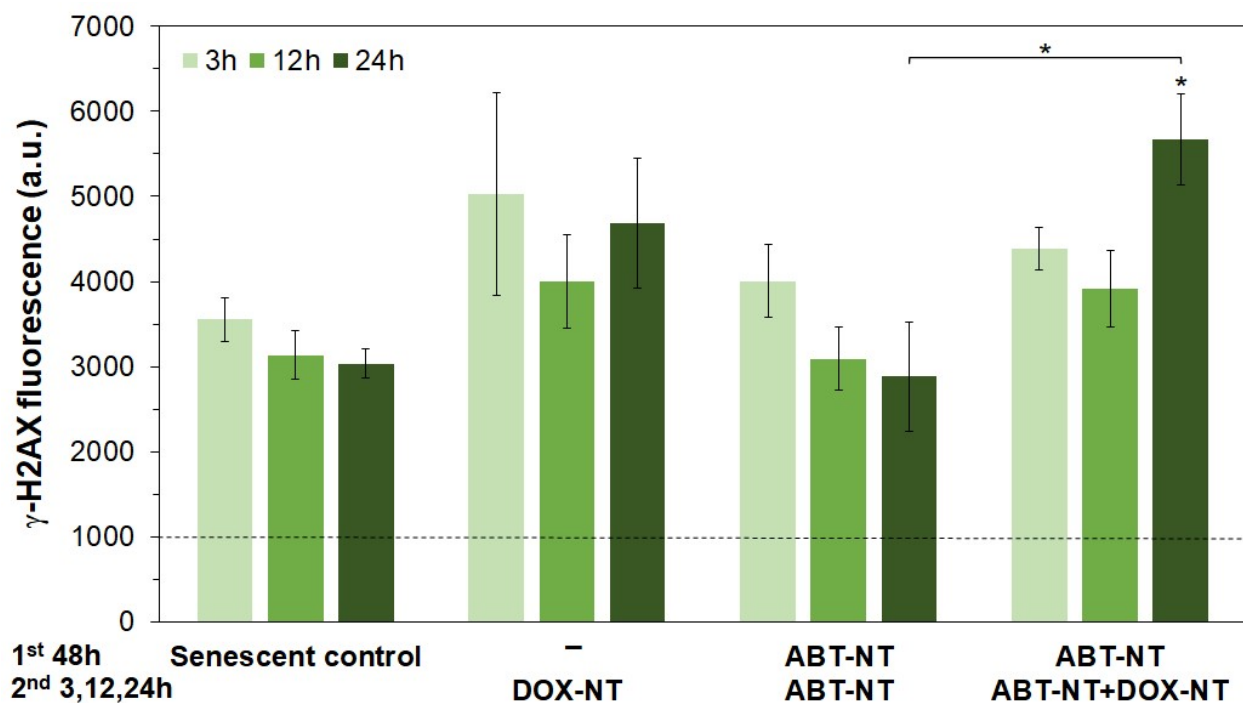


Fig. S9 Detection of γ -H2AX via flow cytometry. MDA-MB-231 cells made senescent through treatment with 0.05 $\mu\text{g}/\text{mL}$ DOX for 3 days at 37 $^{\circ}\text{C}$. DOX-NT (0.5 $\mu\text{g}/\text{mL}$ DOX), ABT-NT (0.1 μM ABT-263) or the combination of the two was delivered to cells according to the treatment scheme detailed below the graph. Longer times were not pursued for the 2nd treatment as there were not enough viable cells for analysis. The dotted line shows the expression of γ -H2AX by proliferating cells. Data are shown as mean \pm SD ($n = 3$). Statistical significance between groups at each time point was assessed via one-way ANOVA with post-hoc Tukey's HSD test and symbols directly over bars represent significance compared to untreated samples (senescent control); * $p < 0.05$, for all other groups † $p > 0.05$.